Nat Cell Biol. Author manuscript; available in PMC 2011 November 1.

Published in final edited form as:
Nat Cell Biol. 2010 August ; 12(8): 791–798. doi:10.1038/ncb2083.

A spindle-like apparatus guides bacterial chromosome segregation

Jerod L. Ptacin[1], **Steven F. Lee**[2], **Ethan C. Garner**[3], **Esteban Toro**[1], **Michael Eckart**[4], **Luis R. Comolli**[5], **W.E. Moerner**[2], and **Lucy Shapiro**[1]

[1]Department of Developmental Biology, Stanford University School of Medicine, Beckman Center, Stanford, CA 94305, USA

[2]Department of Chemistry, Stanford University, Stanford, CA 94305, USA

[3]Department of Systems Biology, Harvard Medical School, Boston, MA 02115, USA

[4]Stanford Protein and Nucleic Acid Facility, Stanford University School of Medicine, Beckman Center, Stanford, CA 94305, USA

[5]Life Sciences Division, Lawrence Berkeley National Laboratory, Berkeley, CA 94720, USA

Abstract

Until recently, a dedicated mitotic apparatus that segregates newly replicated chromosomes into daughter cells was believed to be unique to eukaryotic cells. Here we demonstrate that the bacterium *Caulobacter crescentus* segregates its chromosome using a partitioning (Par) apparatus that has surprising similarities to eukaryotic spindles. We show that the *C. crescentus* ATPase ParA forms linear polymers *in vitro* and assembles into a narrow linear structure *in vivo*. The centromere-binding protein ParB binds to and destabilizes ParA structures *in vitro*. We propose that this ParB-stimulated ParA depolymerization activity moves the centromere to the opposite cell pole through a burnt bridge Brownian ratchet mechanism. Finally, we identify the pole-specific TipN protein[1,2] as a new component of the Par system that is required to maintain the directionality of DNA transfer towards the new cell pole. Our results elucidate a bacterial chromosome segregation mechanism that features basic operating principles similar to eukaryotic mitotic machines, including a multivalent protein complex at the centromere that stimulates the dynamic disassembly of polymers to move chromosomes into daughter compartments.

Recent evidence suggests that *Caulobacter crescentus* and other bacteria use DNA partitioning (Par) systems related to those found in plasmids to segregate chromosomal origin regions on DNA replication. Par systems are found throughout bacterial species[3] and consist of three core components: 1) an origin-proximal centromeric DNA sequence, *parS*;

Correspondence should be addressed to L.S. (shapiro@stanford.edu).

Supplementary Information is available on the Nature Cell Biology website.

AUTHOR CONTRIBUTIONS

J.P., S.L., W.E.M. and L.S. designed the research; J.P. performed *C. crescentus* genetic, epifluorescence microscopy and biochemical experiments; S.L. performed single molecule imaging and data analysis; E.G. purified native ParA and performed ParA light-scattering experiments; E.T. designed ParA/DNA SPR experiments and performed time-lapse microscopy experiments on Δ*tipN* strains; M.E. performed SPR experiments and analysis; L.C. performed ParA negative-stain electron microscopy imaging; W.E.M. and L.S. supervised the study; J.P., S.L., W.E.M. and L.S. wrote the paper.

COMPETING INTERESTS

The authors declare no competing financial interests.

2) an ATPase ParA, hypothesized to provide the force for centromere segregation through dynamic polymerization; and 3) a mediator protein ParB, which binds to *parS* and is predicted to regulate and couple ParA-induced force to *parS* movement. In *C. crescentus*, ParA and ParB are essential[4]. Depletion of ParB, overexpression of ParA and/or ParB, extra *parS* sequences, or mutations in the ParA ATPase active site result in severe chromosome segregation defects[4–6]. Furthermore, the *C. crescentus parS* site has been identified as the functional centromere[6], and blocking DNA replication initiation prevents translocation of the ParB–*parS* complex to the opposite cell pole[7]. In addition to the core Par components, *C. crescentus* uses a pole-specific protein PopZ to tether the *parS* region to the pole through direct interaction with ParB, which prevents reverse segregation of the ParB–*parS* complex[8,9]. Together, these data suggest that the *C. crescentus* Par system, in cooperation with the polar PopZ network, mediates the active segregation and subsequent tethering of the *parS* region to the cell pole to initiate chromosome partitioning.

Despite a clear role in DNA partitioning, the mechanisms proposed for Par systems are diverse and largely hypothetical[10–16]. However, Par systems have several common features. Various ParA homologues have been shown to polymerize *in vitro*[10,11,16–20]. Dynamic pole-to-pole oscillation of ParA localization has been observed *in vivo,* and in some cases has been shown to require ATPase activity and the presence of both ParB and *parS*[10,12,13,15,19,21–25]. Importantly, recent observations demonstrate a correlation between ParB movement and a retracting cloud-like localization of ParA during segregation[12,15], suggesting that a ParA structure ‘pulls’ ParB–*parS* complexes. However, the architecture of ParA assemblies, the molecular mechanisms by which these structures form and generate chromosomal movement, and the cellular components required to impart directionality to ParA-mediated segregation have yet to be established.

To examine the role of ParA and ParB in chromosome segregation, we replaced the *C. crescentus* chromosomal *parA* and *parB* genes with *parA-eyfp* and *cfp-parB*, respectively, and used time-lapse microscopy to image synchronized cells. Initially CFP–ParB bound to *parS* formed a focus (red) at the old pole, as reported previously[5], and ParA–eYFP (green) localized predominantly between the new pole and the CFP–ParB focus (Fig. 1a). Next, the CFP–ParB focus duplicated, and one focus followed the edge of a receding ParA–eYFP structure towards the opposite cell pole (Fig. 1a, top row; Supplementary Information, Fig. S1a), suggesting that a retracting ParA complex moves ParB–*parS* during segregation[12,15].

To obtain higher resolution images of ParA *in vivo*, we performed two-colour single-molecule fluorescence imaging to extract super resolution images of ParA–eYFP and mCherry–ParB localizations during segregation in live cells. Figure 1b shows representative epifluorescence and super resolution images of ParA–eYFP (green) and mCherry–ParB (red) in cells at different stages of *parS* progression towards the distal pole. We observed that ParA–eYFP molecules localized to a discrete linear structure (Fig. 1b; Supplementary Information, Fig. S1a and b) with widths of 40.1 ± 9.5 nm. A cell imaged before replication initiation (Fig. 1b, cell A), shows a linear ParA–eYFP structure. Cells imaged during segregation (Fig. 1b, cell B) show linear ParA–eYFP assemblies that frequently have the highest density of ParA localizations between the new pole and the segregating ParB–*parS* complex, reflecting at super resolution the retracting cloud-like ParA localizations in the epifuorescence images in Fig. 1a (Supplementary Information, Fig. S1b). Finally, cells imaged after the completion of *parS* segregation (Fig. 1b, cell C) show linear ParA structures that stretch from pole to pole, suggesting reorganization of the ParA structure after segregation. No ordered assemblies were observed when we imaged cytoplasmic eYFP alone, but linear ParA–eYFP structures were observed in cells after fixing with formaldehyde (Supplementary Information, Fig. S1c) and when ParA was fused to mCherry (Supplementary Information, Fig. S1c). To further demonstrate the consistency between the epifluorescence and super resolution experiments, we reconstructed diffraction-limited images using the super resolution fitted localization data (Supplementary Information, Fig. S1d) that matched well with the epifluorescence images (Fig. 1a). We conclude that ParA–eYFP is assembled predominantly into a narrow linear structure oriented along the long axis of the cell, which could not be resolved with diffraction-limited microscopy.

The narrow linear structures of ParA–eYFP observed *in vivo* suggest that these structures consist of ParA polymers. We therefore purified ParA and measured multimerization using light scattering (Supplementary Information, Fig. S2a). ParA combined with ATP produced a rapid increase in light scattering, indicating polymerization (green). No increase in light scattering was observed in the absence of nucleotide, and ADP stimulated a slow increase (blue and red, respectively). We imaged ParA structures directly using negative-stain electron microscopy. When incubated without ATP, no ParA polymers were observed (Supplementary Information, Fig. S2b). However, in the presence of ATP, ParA formed linear polymers that were laterally bundled (Fig. 1c, upper and lower panels), as observed for other ParA homologues[10,11,16,17,19].

We performed a mutational analysis to determine the roles of ParA biochemical interactions in ParA localization. The proposed ParA biochemical pathway[18] is shown in Fig. 2a. Apo–ParA binds to ATP (Fig. 2a, top), stimulating ParA homodimerization[18,19]. The ATP-bound ParA dimer interacts with ParB, binds to DNA, or polymerizes[18,19]. ParB stimulates ParA ATP hydrolysis[11,19,26] or nucleotide exchange[27], releasing ParA as monomers (Fig. 2a, bottom). We mutated conserved ParA residues to abrogate specific biochemical interactions (Fig. 2a; Supplementary Information, Fig. 2c–e) and observed the localizations in *C. crescentus* using fluorescence microscopy (Fig. 2b). Wild-type ParA–eYFP localized as a retracting 'comet'-like structure (Figs 1a, 2b). An ATP-binding mutant, $ParA^{K20Q}$ ($ParA_{binding}$)[12,13,18,22,23,28] localized diffusely with puncta at the new pole (Fig. 2b). A ParA dimerization mutant, $ParA^{G16V}$ ($ParA_{dimer}$)[18,23,29], localized diffusely and in bipolar foci (Fig. 2b), and an ATP hydrolysis mutant, $ParA^{D44A}$ ($ParA_{hydrolysis}$)[18,29], colocalized with ParB foci and in patches throughout the cell (Fig. 2b). Localization of ParA proteins that contained a $ParA_{binding}$ mutation, combined with a $ParA_{dimer}$ or a $ParA_{hydrolysis}$ mutation, was identical to that of the $ParA_{binding}$ mutant alone (Supplementary Information, Fig. S3f). Similarly, localization of a ParA protein that contained a $ParA_{dimer}$ mutation, combined with a $ParA_{hydrolysis}$ mutation, was indistinguishable from that of the single $ParA_{dimer}$ mutant (Supplementary Information, Fig. S3f), consistent with the proposed hierarchy.

We assessed the role of nucleoid binding in ParA localization. We created a DNA-binding mutant, $ParA^{R195E}$ ($ParA_{DNA}$)[11,25,30], and found that it localized exclusively in foci at the cell poles (Fig. 2b), suggesting a role for DNA binding in ParA localization. To further examine ParA DNA binding, we observed the localizations of ParA–eYFP mutants in *Escherichia coli* (Fig. 2c), which does not contain a Par system[3] but has prominent nucleoid masses. In *E. coli,* $ParA_{binding}$–eYFP, $ParA_{dimer}$–eYFP and $ParA_{DNA}$–eYFP all localized diffusely (Fig. 2c). By contrast, wild-type ParA–eYFP and $ParA_{hydrolysis}$–eYFP localized in patches along the nucleoid (Fig. 2c and data not shown), supporting the requirements of ATP binding and dimerization for ParA interaction with DNA.

To directly examine the biochemical requirements for ParA interaction with ParB and with DNA, we used surface plasmon resonance (SPR). When we immobilized ParB and added ParA and ATP, we observed a rapid increase in response (Fig. 2d). ParA injected with ADP or without nucleotide produced a minimal response (Fig. 2d). We next immobilized the non-specific DNA duplex, *parS-scr*[8], and assessed ParA association. ParA produced an increase in response when combined with ATP (Fig. 2e). On its own, or when combined with ADP, ParA produced a minimal response (Fig. 2e), suggesting that ATP is required for ParA polymerization and its interaction with ParB and with DNA.

As ParA readily binds DNA *in vitro* and *in vivo*, we hypothesized that nucleoid-immobilized ParA structures move the ParB-bound centromere complex through ParB-stimulated dissociation of ParA subunits from the DNA. We examined the role of ParB in ParA dynamics by localizing ParA–eYFP in ParB-depleted cells. After ParB depletion, ParA localized uniformly throughout the cell, whereas dynamic ParA–eYFP structures were observed in cells not depleted of ParB (Fig. 3a). In cells depleted of wild-type ParB, but expressing mCherry–ParB, ParA–eYFP localization was dynamic and led mCherry–ParB foci poleward (Fig. 3a). However, expression of a ParA interaction-deficient mutant, $\mathrm{ParB}^{\mathrm{L12A}}$ (ref. 32; Supplementary Information, Fig. S3a) produced static mCherry–ParB foci and diffuse ParA–eYFP localization (Fig. 3a). To dissect the role of *parS*, we localized ParA and ParB in *E. coli* cells with and without a *parS*-containing plasmid. ParA–eYFP expressed with or without the *parS* plasmid localized to the nucleoid (Fig. 3b). CFP–ParB expressed alone localized diffusely without *parS*, but formed foci in the presence of the *parS* plasmid (Fig. 3b). Co-expressed ParA–eYFP and CFP–ParB localized similarly to the single expression strains without *parS*, but in the presence of *parS*, CFP–ParB formed foci and ParA–eYFP occasionally oscillated between nucleoids (Fig. 3b, c). These results suggest that, *in vivo*, ParB clustered on *parS* stimulates the dynamic localization of ParA structures over the nucleoid.

We tested the effect of ParB on the stability of ParA–DNA complexes *in vitro* using SPR. When associated with a nonspecific DNA surface, ParA with ATP produced a rapid increase in response, followed by a slow dissociation with buffer only (Fig. 3d). When ParB was injected during ParA dissociation, we observed an abrupt increase in response, indicating the formation of a ParB complex with DNA-bound ParA. Subsequently, the signal rapidly decreased to well below the ParA dissociation curve, indicating the dissociation of ParA from the DNA (Fig. 3d, red). Similar results were observed using gel shifts (Supplementary Information, Fig. S3b). These data suggest that the ParB–*parS* complex moves relative to the ParA-bound nucleoid through simultaneous binding to and removal of ParA from the structure.

The *C. crescentus* ParA dynamics observed in *E. coli* suggest that ParA, ParB and *parS* are sufficient to assemble a dynamic machine. However, the polar localization of ParA mutants in *C. crescentus* (Fig. 2b) suggests that additional factors contribute to ParA localization. To identify polar interaction partners of ParA, we expressed the bipolar-localized $\mathrm{ParA}_{\mathrm{DNA}}$–eYFP in strains with deletions in proteins known to localize to the new cell pole. In cells lacking the new pole protein TipN[1,2], we observed a decrease in the frequency of new-pole $\mathrm{ParA}_{\mathrm{DNA}}$–eYFP foci (data not shown), suggesting that TipN is required to position $\mathrm{ParA}_{\mathrm{DNA}}$. To examine the role of TipN in segregation, we visualized ParB–*parS* segregation in synchronized wild-type (JP138) and Δ*tipN* (JP141) strains. The JP138 strain had a similar efficiency of chromosome segregation as that observed for the *parB::cfp-parB* strain (Fig. 4a). However, the Δ*tipN* strain showed predominantly partial *parS* segregation events (Fig. 4a). Time-lapse imaging of ParA–eYFP and mCherry–ParB in Δ*tipN* showed that ParB–*parS* translocation paused frequently and reversed direction (Fig. 4b; Supplementary Information, Fig. S3c). Reversal correlated with ParA redistribution to the opposite side of the ParB–*parS* complex (Fig. 4b; Supplementary Information, Fig. S3c). Therefore, TipN is required to maintain ParA-mediated *parS* translocation directionality towards the new pole.

To determine whether ParA and TipN interact directly, we developed an assay to screen for protein–protein interactions in *E. coli*. This assay used a peptide from the *Shigella* protein IcsA ($\mathrm{IcsA}_{507–620}$, hereafter referred to as IcsA) to localize proteins to the *E. coli* cell pole[33], allowing colocalization studies with other fluorescent proteins. Full-length *C. crescentus* TipN fused to IcsA localized to the *E. coli* pole and recruited $\mathrm{ParA_{DNA}}$–eYFP (Fig. 4c), whereas IcsA alone did not (data not shown). IcsA fusions to both the TipN N-terminal domain ($\mathrm{TipN_{NTD}}$, residues 1–207) and the C-terminal domain ($\mathrm{TipN_{CTD}}$, residues 205–888) also localized to the cell pole, but only the $\mathrm{TipN_{CTD}}$ recruited $\mathrm{ParA_{DNA}}$–eYFP (Fig. 4c). We assayed the direct interaction of ParA with immobilized using $\mathrm{TipN_{CTD}}$ *in vitro* SPR. On addition of ParA and ATP, we observed an increase in signal corresponding to ParA binding that was specific for $\mathrm{TipN_{CTD}}$ (Fig. 4d). ParA and ADP, or no nucleotide, produced a lower signal than that observed with ATP (Fig. 4d), suggesting that apo-ParA interacts directly with the C-terminal region of TipN, and that ATP augments the interaction.

Together, our data support a burnt-bridge Brownian ratchet model for Par-mediated chromosome segregation in *C. crescentus* (Fig. 5a, b). *In vitro*, ParA formed linear polymers, but also interacted readily with DNA *in vitro* and *in vivo*, suggesting that ParA polymers may form either along the nucleoid or freely in the cytoplasm, or both, and bundle into a linear structure (Fig. 5a, vi). *In vitro*, ParB removes ParA from DNA, consistent with our observations *in vivo* that ParB depletion or mutation quenches ParA dynamics, and that wild-type ParB complexes ‘follow’ a receding ParA structure. Thus, we propose that ParB stimulates the dissociation of ParA subunits from the ends of a ParA structure while remaining attached, moving the ParB-*parS* complex along a retracting ParA structure (Fig. 5a, vii). The simultaneous interaction with, and dissociation of, the ParA structure may be explained by the association of multiple ParB proteins with the *parS* region[34,35]. Thermal motion of the ParB-*parS* complex may be trapped by ParB binding to the ParA structure as the structure shortens, explaining the rectified diffusional motion observed for ParB complexes in *Vibrio cholerae*[36]. Finally, our data suggest that ParB-*parS* complexes move along a subset of fibres within the ParA bundle, as a less intense structure is often left behind the translocating ParB complex. Thus, ParA may be available for ParB-stimulated removal only when located at protofilament termini.

The *C. crescentus* Par system mobilizes the *parS* locus unidirectionally from the old pole to the new pole[37], in contrast to the bidirectional movement observed for plasmid segregation[15]. One contributor to unidirectionality in *C. crescentus* is the polar protein PopZ, which tethers ParB-*parS* to the cell pole[8,9] (Fig. 5b, i) to prevent reversals. Here we identify a new directionality factor for the *C. crescentus* Par system: the new pole-specific protein TipN[1,2]. Without TipN, ParA localizes aberrantly, causing pauses and reversals in ParB–*parS* segregation. These defects observed in the absence of *tipN* may reflect secondary effects, such as on the MreB-associated cytoskeleton[1]. However, ParA and TipN interact directly *in vitro* (Fig. 4d), suggesting a functional interaction *in vivo*. TipN might nucleate or stabilize ParA structures at the new pole (Fig. 5b, i). Alternatively, TipN might simply provide a binding site for ParA to increase the local concentration and bias the insertion of free ParA molecules into the structure at the new pole. After segregation, the translocated ParB–*parS* complex is anchored to PopZ at the new pole (Fig. 5b, v), while TipN is recruited to the division plane to remain at the new poles of the daughter cells to reset the cycle.

Overall, the basic operating principles that drive DNA segregation seem to be shared between prokaryotic and eukaryotic mitotic machineries. The bacterial ParB–*parS* complex shares functional and architectural similarities with the eukaryotic kinetochore complexes, as both associate with, and spread along, the centromere DNA region[38]. Both *C. crescentus* and eukaryotic kinetochores seem to use multivalent attachments to allow the simultaneous binding to, and depolymerization of, the polymers that guide their movement, reminiscent of the eukaryotic DamI–Ndc80 complex proposed to follow along depolymerizing microtubule ends[38]. Finally, polar TipN may function as a centrosome-like organization centre to bias the movement of retracting polymers towards the cell pole.

METHODS

Methods and any associated references are available in the online version of the paper at http://www.nature.com/naturecellbiology/

Supplementary Material

Refer to Web version on PubMed Central for supplementary material.

Acknowledgments

We thank Jimmy Blair for assistance with modelling of ParA mutants, and critical reading of the manuscript; and Grant Bowman, Erin Goley and Julie Biteen for technical advice. We thank Jian Zhu and Thomas Earnest for providing purified 6His–ParB. This work is supported by National Institutes of Health grants R01 GM51426 R24 and GM073011-04d to L.S., NIH/NIGMS fellowship F32GM088966-1 to J.P., NIH/NIGMS award R01GM086196-2 to W.E.M., the Smith Stanford Graduate Fellowship to E.T., and a Helen Hay Whitney postdoctoral fellowship to E.G. This work was also supported by the Director, Office of Science, Office of Biological and Environmental Research, of the U.S. Department of Energy under contract no. DE-AC02-05CH11231.

References

1. Lam H, Schofield WB, Jacobs-Wagner C. A landmark protein essential for establishing and perpetuating the polarity of a bacterial cell. Cell. 2006; 124:1011–1023. [PubMed: 16530047]
2. Huitema E, Pritchard S, Matteson D, Radhakrishnan SK, Viollier PH. Bacterial birth scar proteins mark future flagellum assembly site. Cell. 2006; 124:1025–1037. [PubMed: 16530048]
3. Gerdes K, Moller-Jensen J, Bugge Jensen R. Plasmid and chromosome partitioning: surprises from phylogeny. Mol Microbiol. 2000; 37:455–466. [PubMed: 10931339]
4. Mohl DA, Easter J Jr, Gober JW. The chromosome partitioning protein, ParB, is required for cytokinesis in *Caulobacter crescentus*. Mol Microbiol. 2001; 42:741–755. [PubMed: 11722739]
5. Mohl DA, Gober JW. Cell cycle-dependent polar localization of chromosome partitioning proteins in *Caulobacter crescentus*. Cell. 1997; 88:675–684. [PubMed: 9054507]
6. Toro E, Hong SH, McAdams HH, Shapiro L. *Caulobacter* requires a dedicated mechanism to initiate chromosome segregation. Proc Natl Acad Sci USA. 2008; 105:15435–15440. [PubMed: 18824683]
7. Bowman GR, et al. *Caulobacter* PopZ forms a polar subdomain dictating sequential changes in pole composition and function. Mol Microbiol. 76:173–189. [PubMed: 20149103]
8. Bowman GR, et al. Polymeric protein anchors the chromosomal origin/ParB complex at a bacterial cell pole. Cell. 2008; 134:945–955. [PubMed: 18805088]
9. Ebersbach GBA, Jensen GJ, Jacobs-Wagner C. A self-associating protein critical for chromosome attachment, division, and polar organization in *Caulobacter*. Cell. 2008; 134:956–968. [PubMed: 18805089]
10. Lim GE, Derman AI, Pogliano J. Bacterial DNA segregation by dynamic SopA polymers. Proc Natl Acad Sci USA. 2005; 102:17658–17663. [PubMed: 16306264]
11. Bouet JY, Ah-Seng Y, Benmeradi N, Lane D. Polymerization of SopA partition ATPase: regulation by DNA binding and SopB. Mol Microbiol. 2007; 63:468–481. [PubMed: 17166176]
12. Fogel MA, Waldor MK. A dynamic, mitotic-like mechanism for bacterial chromosome segregation. Genes Dev. 2006; 20:3269–3282. [PubMed: 17158745]
13. Hatano T, Yamaichi Y, Niki H. Oscillating focus of SopA associated with filamentous structure guides partitioning of F plasmid. Mol Microbiol. 2007; 64:1198–1213. [PubMed: 17542915]
14. Leonard TA, Moller-Jensen J, Lowe J. Towards understanding the molecular basis of bacterial DNA segregation. Philos Trans R Soc Lond B Biol Sci. 2005; 360:523–535. [PubMed: 15897178]

15. Ringgaard S, van Zon J, Howard M, Gerdes K. Movement and equipositioning of plasmids by ParA filament disassembly. Proc Natl Acad Sci USA. 2009; 106:19369–19374. [PubMed: 19906997]

16. Barilla D, Rosenberg MF, Nobbmann U, Hayes F. Bacterial DNA segregation dynamics mediated by the polymerizing protein ParF. EMBO J. 2005; 24:1453–1464. [PubMed: 15775965]

17. Ebersbach G, et al. Regular cellular distribution of plasmids by oscillating and filament-forming ParA ATPase of plasmid pB171. Mol Microbiol. 2006; 61:1428–1442. [PubMed: 16899080]

18. Leonard TA, Butler PJ, Lowe J. Bacterial chromosome segregation: structure and DNA binding of the Soj dimmer — a conserved biological switch. EMBO J. 2005; 24:270–282. [PubMed: 15635448]

19. Pratto F, et al. *Streptococcus pyogenes* pSM19035 requires dynamic assembly of ATP-bound ParA and ParB on parS DNA during plasmid segregation. Nucleic Acids Res. 2008; 36:3676–3689. [PubMed: 18477635]

20. Batt SM, Bingle LE, Dafforn TR, Thomas CM. Bacterial genome partitioning: N-terminal domain of IncC protein encoded by broad-host-range plasmid RK2 modulates oligomerisation and DNA binding. J Mol Biol. 2009; 385:1361–1374. [PubMed: 19109978]

21. Ebersbach G, Gerdes K. The double par locus of virulence factor pB171: DNA segregation is correlated with oscillation of ParA. Proc Natl Acad Sci USA. 2001; 98:15078–15083. [PubMed: 11752455]

22. Ebersbach G, Gerdes K. Bacterial mitosis: partitioning protein ParA oscillates in spiral-shaped structures and positions plasmids at mid-cell. Mol Microbiol. 2004; 52:385–398. [PubMed: 15066028]

23. Quisel JD, Lin DC, Grossman AD. Control of development by altered localization of a transcription factor in *B. subtilis*. Mol Cell. 1999; 4:665–672. [PubMed: 10619014]

24. Marston AL, Errington J. Dynamic movement of the ParA-like Soj protein of *B. subtilis* and its dual role in nucleoid organization and developmental regulation. Mol Cell. 1999; 4:673–682. [PubMed: 10619015]

25. Castaing JP, Bouet JY, Lane D. F plasmid partition depends on interaction of SopA with non-specific DNA. Mol Microbiol. 2008; 70:1000–1011. [PubMed: 18826408]

26. Barilla D, Carmelo E, Hayes F. The tail of the ParG DNA segregation protein remodels ParF polymers and enhances ATP hydrolysis via an arginine finger-like motif. Proc Natl Acad Sci USA. 2007; 104:1811–1816. [PubMed: 17261809]

27. Easter J Jr, Gober JW. ParB-stimulated nucleotide exchange regulates a switch in functionally distinct ParA activities. Mol Cell. 2002; 10:427–434. [PubMed: 12191487]

28. Fung E, Bouet JY, Funnell BE. Probing the ATP-binding site of P1 ParA: partition and repression have different requirements for ATP binding and hydrolysis. EMBO J. 2001; 20:4901–4911. [PubMed: 11532954]

29. Murray H, Errington J. Dynamic control of the DNA replication initiation protein DnaA by Soj/ParA. Cell. 2008; 135:74–84. [PubMed: 18854156]

30. Hester CM, Lutkenhaus J. Soj (ParA) DNA binding is mediated by conserved arginines and is essential for plasmid segregation. Proc Natl Acad Sci USA. 2007; 104:20326–20331. [PubMed: 18077387]

31. Thanbichler M, Shapiro L. MipZ, a spatial regulator coordinating chromosome segregation with cell division in *Caulobacter*. Cell. 2006; 126:147–162. [PubMed: 16839883]

32. Gruber S, Errington J. Recruitment of condensin to replication origin regions by ParB/SpoOJ promotes chromosome segregation in *B. subtilis*. Cell. 2009; 137:685–696. [PubMed: 19450516]

33. Charles M, Perez M, Kobil JH, Goldberg MB. Polar targeting of *Shigella* virulence factor IcsA in *Enterobacteriacae* and *Vibrio*. Proc Natl Acad Sci USA. 2001; 98:9871–9876. [PubMed: 11481451]

34. Breier AM, Grossman AD. Whole-genome analysis of the chromosome partitioning and sporulation protein Spo0J (ParB) reveals spreading and origin-distal sites on the *Bacillus subtilis* chromosome. Mol Microbiol. 2007; 64:703–718. [PubMed: 17462018]

35. Rodionov O, Lobocka M, Yarmolinsky M. Silencing of genes flanking the P1 plasmid centromere. Science. 1999; 283:546–549. [PubMed: 9915704]

36. Fiebig A, Keren K, Theriot JA. Fine-scale time-lapse analysis of the biphasic, dynamic behaviour of the two *Vibrio cholerae* chromosomes. Mol Microbiol. 2006; 60:1164–1178. [PubMed: 16689793]

37. Viollier PH, et al. Rapid and sequential movement of individual chromosomal loci to specific subcellular locations during bacterial DNA replication. Proc Natl Acad Sci USA. 2004; 101:9257–9262. [PubMed: 15178755]

38. Tanaka TU, Desai A. Kinetochore-microtubule interactions: the means to the end. Curr Opin Cell Biol. 2008; 20:53–63. [PubMed: 18182282]

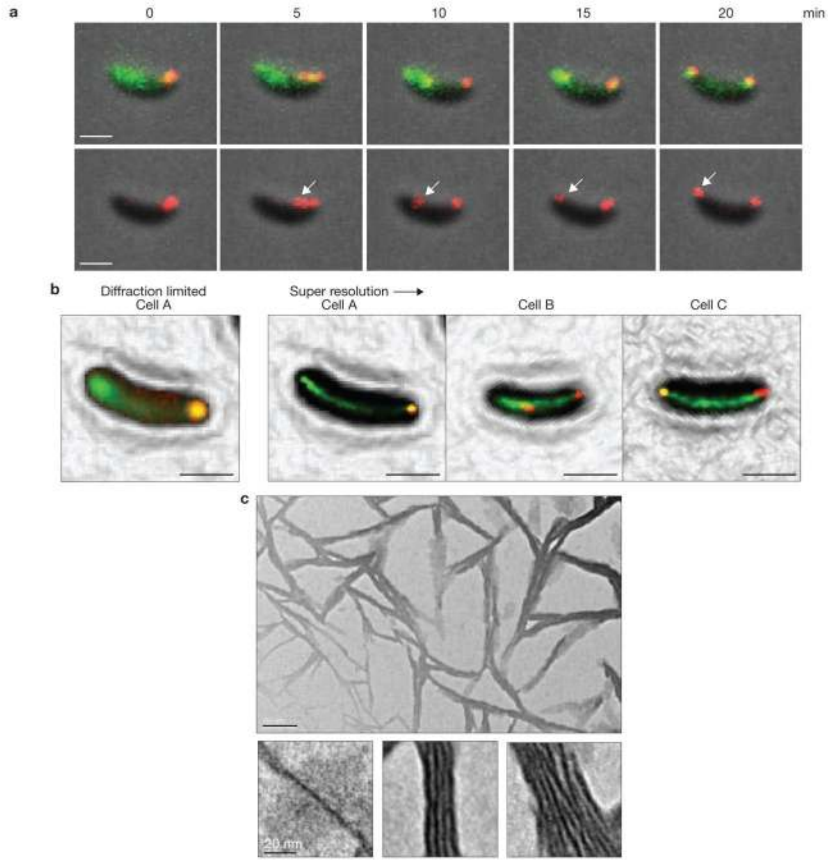

Figure 1.

ParA and ParB dynamics *in vivo* and ParA polymerization *in vitro* suggest a retracting polymeric ParA structure guides centromere segregation. (**a**) A retracting ParA structure leads the ParB–*parS* complex towards the new pole. Time-lapse epifluorescence microscopy of JP110 swarmer cells imaged at 5-min intervals on initiation of S phase. Phase-contrast, ParA–eYFP (green) and CFP–ParB (red) images (top row), or phase and CFP–ParB images (bottom row) are overlaid. The translocating CFP–ParB-bound *parS* complex is indicated (white arrow). Scale bars, 1 µm. (**b**) Super-resolution imaging reveals that the retracting 'cloud'-like ParA in epifluorescence images corresponds to a narrow linear ParA structure. Representative images of JP138 cells at various stages of *parS* segregation are shown: a diffraction-limited epifluorescence image and corresponding super resolution image of a representative cell (cell A); a cell undergoing *parS* segregation (Cell B); and a cell after *parS* segregation is completed (cell C). For the super resolution images, the locations of ParA–eYFP (green) and CFP–ParB (red) molecules are plotted as 2D Gaussians with width defined by the fit error of the single-molecule localizations, and overlaid with the white light cell outline. Scale bars, 1 µm. (**c**) Purified ParA polymerizes in the presence of ATP *in vitro*. A representative negative-stain electron micrograph of ParA incubated with ATP is shown (upper panel; scale bar, 100 nm). Higher magnification images (lower panel; scale bar, 20 nm), showing single (lower left) and bundled ParA protofilaments (lower middle and right).

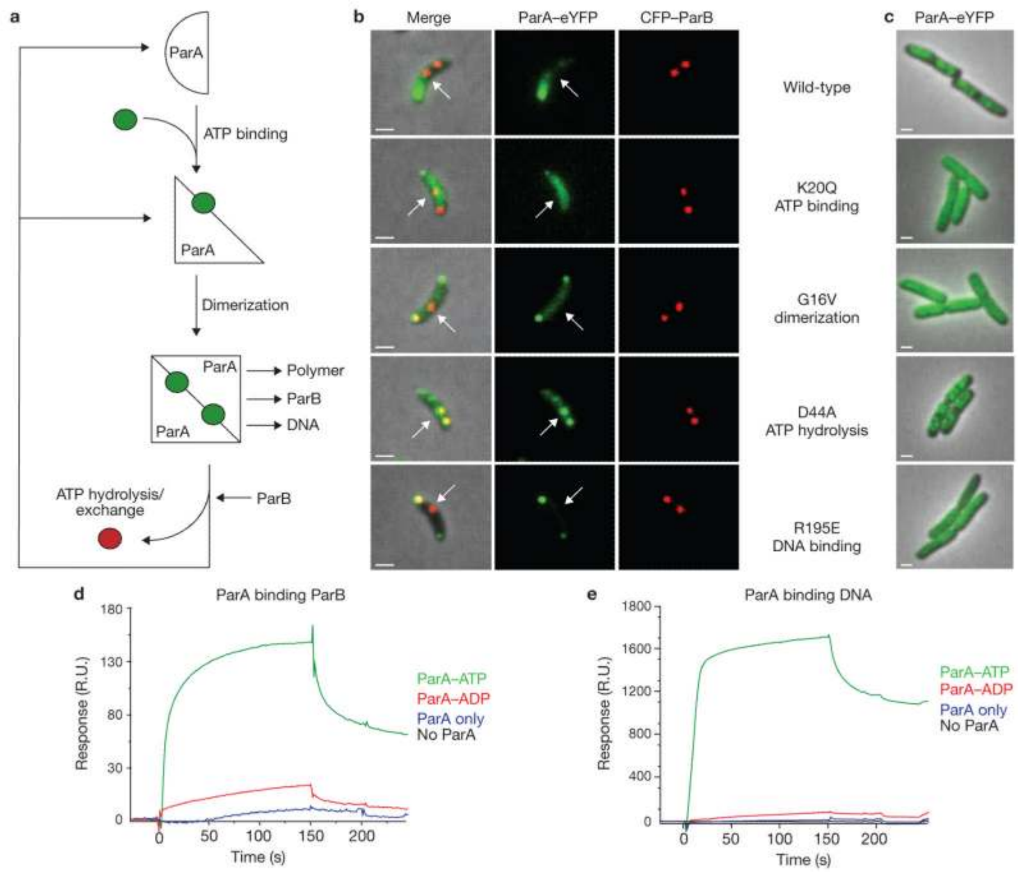

Figure 2.

Mutational and biochemical analysis of *C. crescentus* ParA. (**a**) Consensus view of the ParA biochemical pathway[18]. Apo–ParA (half-circle) binds ATP (green circle), changes conformation (triangle with green circle), and dimerizes[18]. ParB-stimulated ATP hydrolysis or nucleotide exchange of the ParA dimer (square with green circles) causes release of ADP (red circle) and P_i to reset the cycle. (**b**) Images of *C. crescentus* strains expressing merodiploid wild-type or mutant ParA–eYFP. Phase, ParA–eYFP (green) and CFP–ParB (red) are overlaid as shown. White arrows indicate partially translocated ParB foci. Scale bars, 1 μm. (**c**) Images of *E. coli* cells expressing wild-type and mutant *C. crescentus* ParA–eYFP proteins. Phase-contrast and eYFP images (green) are overlaid. Scale bars, 1 μm. (**d**) ParA requires ATP for interaction with ParB. Surface plasmon resonance (SPR) analysis using immobilized ParB. ParA (500 nM) injected with ATP (green), ADP (red), or no nucleotide (blue) at $t = 0$, and buffer only (150 s). Response units (R.U.) are plotted versus time (s). (**e**) ParA requires ATP for non-specific DNA binding. SPR analysis using immobilized non-specific DNA duplex (a scrambled *parS* sequence). ParA (500nM) injected with ATP (green), ADP (red), or no nucleotide (blue) at $t = 0$, and buffer only (150 s). Response units (R.U.) are plotted versus time (s).

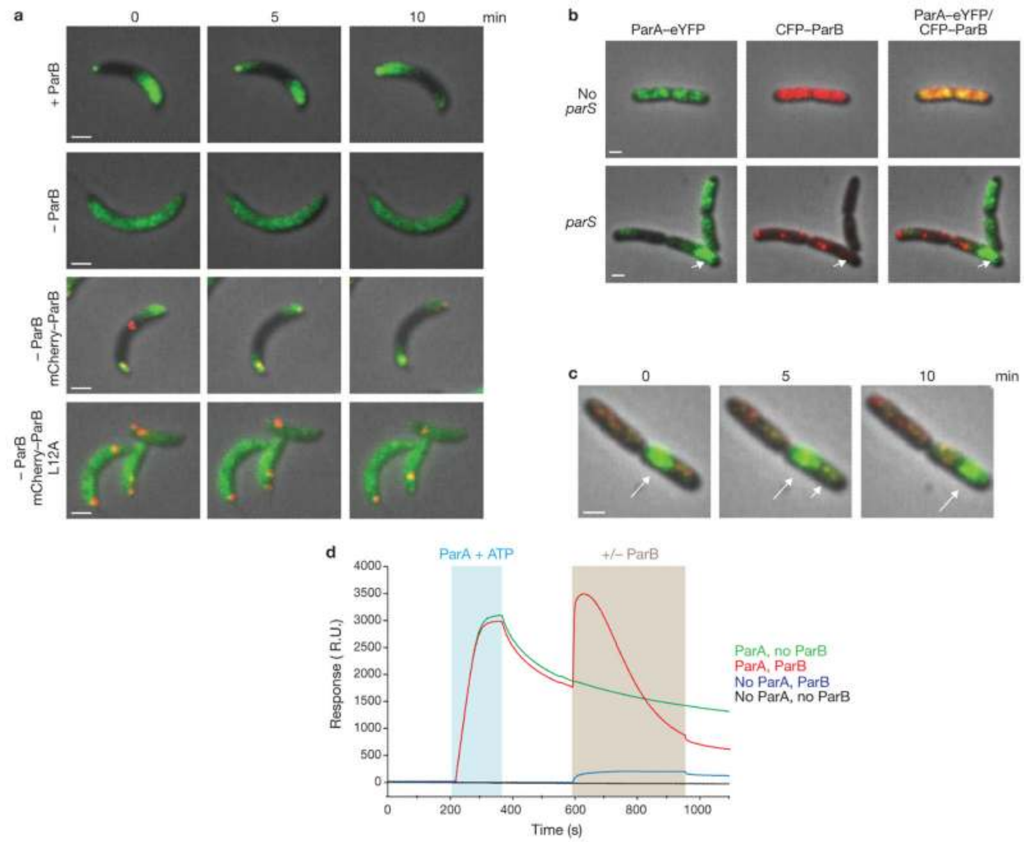

Figure 3.

ParB in complex with *parS* drives the dynamics of ParA structures on DNA. (**a**) ParB is required for the dynamic movement of ParA structures *in vivo. C. crescentus* strains in which the only copy of ParB was controlled by the xylose-inducible promoter were cultured in medium with (+ParB) or without (–ParB) xylose, and induced to express ParA–eYFP (green), or ParA–eYFP and mCherry–ParB (+mCherry–ParB) or mCherry–ParB^{L12A} (+mCherry–ParB^{L12A}; red). Phase and eYFP, or phase/eYFP/mCherry images were collected at 5-min intervals and overlaid as shown. Scale bar, 1 µm. (**b**) ParA localization in *E. coli* requires ParB and *parS* for dynamic movement along the nucleoid. The *E. coli* strains eJP142 (+*parS* plasmid) and eJP140 (–*parS* plasmid) were induced to express CFP–ParB (red) and/or ParA–eYFP (green), and phase, eYFP and CFP images were collected and overlaid as shown. The white arrow indicates dynamic ParA–eYFP localization (see **c**). Scale bar, 1 µm. (**c**) Time-lapse image series of eJP142 cells showing ParA–eYFP localization dynamics. Cultures were prepared as described in **b**, and phase, eYFP and CFP images were collected at 5-min intervals and overlaid. The predominant localization of ParA is indicated with a large white arrow, and smaller arrow indicates other localizations. Scale bar, 1 µm. (**d**) ParB destabilizes a DNA-bound ParA complex *in vitro*. SPR analysis using an immobilized non-specific 162-nucelotide duplex DNA. ParA (375 nM) was first injected with ATP for 150 s (blue region) followed by buffer only for 150 s. Subsequently, 6His–ParB (1 µM dimer, red trace) or buffer only (green trace) was injected for 6 min (grey region) followed by buffer only. The blue trace shows a flow sequence in which no ParA was injected, followed by 6His–ParB (1 µM dimer), showing negligible non-specific DNA binding by 6His–ParB. The black trace represents a flow sequence lacking ParA and 6His–ParB. Response units (R.U.) are plotted against time (s).

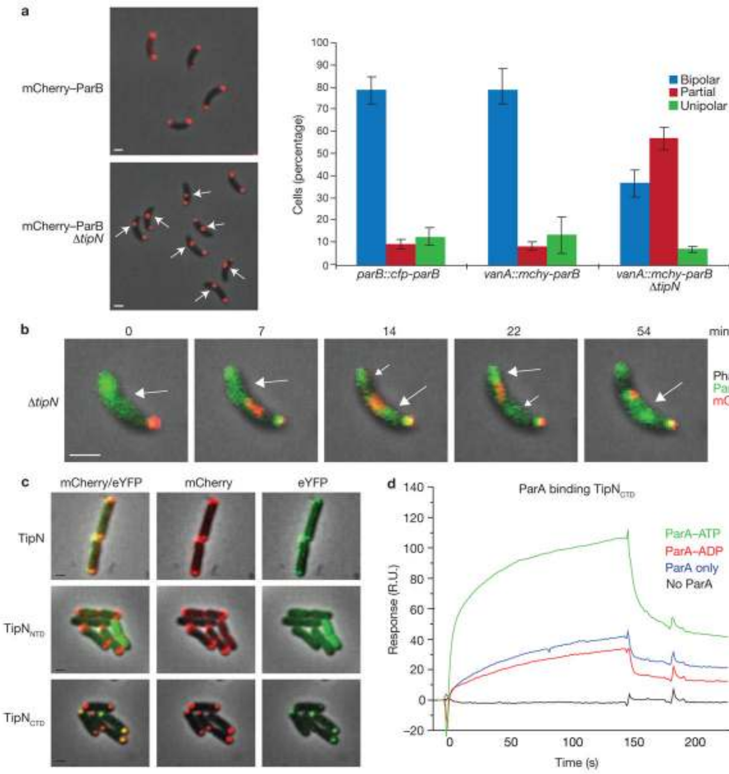

Figure 4.

TipN confers new pole-specific directionality to Par-mediated DNA transfer through direct interaction with ParA. (**a**) Strains lacking *tipN* show severe *parS* segregation defects. Synchronized cultures of JP2 (*parB::cfp-parB*), and of JP138 (*vanA::pvan-mCherry-ParB*) and JP141 (*vanA::pvan-mCherry-ParB, ΔtipN*) were induced to express mCherry–ParB and imaged for phase and mCherry or CFP fluorescence after the initiation of S phase. Representative fields of JP138 (upper left panel) and JP141 (lower left panel) are shown. The white arrows indicate partially segregated ParB–*parS* foci. Scale bar, 1 μm. Mean percentage of cells (right panel) with bipolar ParB foci (blue), unipolar foci (green), or partially translocated foci (red) for JP2, JP138 and JP141. Data are mean ± s.e.m. (n = 3 replicates of >400 cells each). (**b**) Pauses and reversals of ParB–*parS* translocation in the absence of *tipN*. A Δ*tipN* strain was induced to express ParA–eYFP (green) and mCherry–ParB (red). Synchronized and phase-contrast, eYFP and mCherry fluorescence images were collected at the indicated intervals after the initiation of S phase. A representative Δ*tipN* cell undergoing *parS* translocation reversal is shown as phase/eYFP/mCherry overlay. The large white arrows indicate the major ParB-associated ParA localization; smaller arrows indicate other associated ParA structures. Scale bar, 1 μm. (**c**) Heterologous colocalization assay in *E. coli* demonstrates that TipN recruits ParA–eYFP into a complex in *E. coli*. A portion of the *Shigella* protein IcsA (IcsA$_{507–620}$) recruits full-length and fragments of *C. crescentus* TipN to the *E. coli* cell pole. Full-length TipN (top row), TipN$_{NTD}$ (middle row) or TipN$_{CTD}$ (bottom row) fused to IcsA$_{507–620}$–mCherry (red) were co-expressed with ParA$_{DNA}$–eYFP (green) in *E. coli* cells, and imaged for phase contrast, eYFP and mCherry fluorescence. Images are overlaid: phase/mCherry/eYFP (left column), phase/mCherry (middle column), phase/eYFP (right column). fragments. Colocalization is observed only with full-length and TipN$_{CTD}$ (**d**) Purified ParA and TipN$_{CTD}$ interact directly *in vitro*. SPR analysis using immobilized TipN$_{CTD}$. ParA (750 nM) was injected with ATP (green), ADP (red), or no nucleotide (blue), followed by buffer only (150 s). Response units (R.U.) are plotted versus time (s).

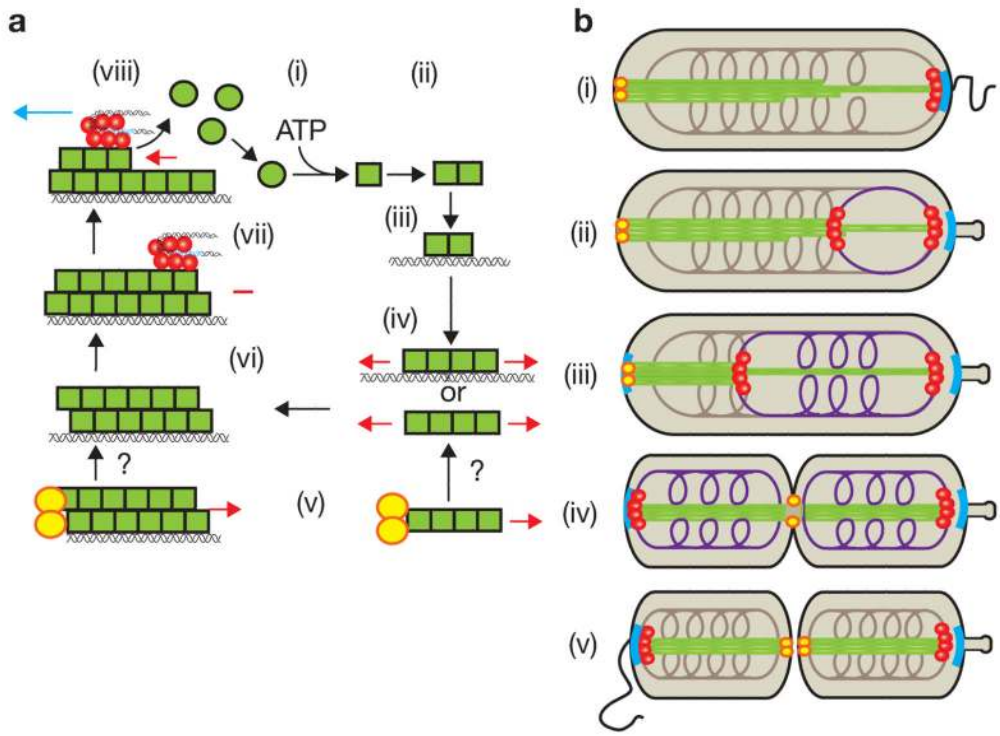

Figure 5.

A burnt-bridge Brownian ratchet mechanism for Par-mediated chromosome segregation in *C. crescentus*. (**a**) Proposed sequence of molecular interactions during Par-mediated DNA segregation. (i) Apo-ParA (green circle) binds ATP, changes conformation (green box), and (ii) dimerizes, (paired green box)[18]. The ParA-ATP homodimer (iii) binds to the nucleoid, or (iv) polymerizes along DNA or in solution (red arrows indicate the direction of polymerization/depolymerization). (v) TipN (yellow circles) may nucleate or stabilize a ParA polymer at the new pole, and (vi) ParA fibres bundle. The ParB–*parS* complex (red circles/blue *parS* DNA) (vii) encounters the end of a ParA fibre and binds. ParB stimulates the terminal ParA of a protofilament to release (viii) and the ParB complex ratchets along the end of a retracting ParA structure (blue arrow indicates direction of ParB–*parS* movement). (**b**) Diagram showing the proposed mechanism operating within the *C. crescentus* cell. (i) A *C. crescentus* swarmer cell. The unreplicated chromosome (brown coil partially associated with ParA) is tethered to the old pole via ParB (red circle) interactions with PopZ (cyan line)[8,9]. TipN (yellow circle) is positioned at the new pole[1,2]. (ii) The ParB–*parS* complex is released from the pole and duplicated *parS* (purple line indicates newly replicated DNA) are decorated with ParB, while TipN may effect the formation or stabilization of a ParA fibre structure (green complex) at the new pole. (iii) A ParB–*parS* complex encounters the ParA structure and binds it. (iv) The ParB–*parS* complex disassembles the ends of some ParA protofilaments, ratcheting along a receding ParA structure, leaving other ParA filaments behind. (v) The ParB–*parS* complex is tethered to the polar PopZ complex. The ParA structure reorganizes, and TipN is recruited to the division site to be positioned for subsequent rounds of segregation.